

Results and Analysis from Mine Impulse Experiments Using Stereo-Digital Image Correlation

**by Craig Barker, Douglas Howle, Terry Holdren, Jeffrey Koch,
and Raquel Ciappi**

ARL-RP-0370

May 2012

**This article appeared in its original form in 26th International Ballistics Symposium, 2011. Lancaster, PA:
DEStech Publications, Inc.**

NOTICES

Disclaimers

The findings in this report are not to be construed as an official Department of the Army position unless so designated by other authorized documents.

Citation of manufacturer's or trade names does not constitute an official endorsement or approval of the use thereof.

Destroy this report when it is no longer needed. Do not return it to the originator.

Army Research Laboratory

Aberdeen Proving Ground, MD 21005

ARL-RP-0370**May 2012**

Results and Analysis from Mine Impulse Experiments Using Stereo-Digital Image Correlation

Craig Barker, Douglas Howle, and Terry Holdren
Survivability/Lethality Analysis Directorate, ARL

Jeffrey Koch
Weapons and Materials Research Directorate, ARL

Raquel Ciappi
SURVICE Engineering Company, 4695 Millennium Dr., Belcamp, MD, 21017

This article appeared in its original form in 26th International Ballistics Symposium, 2011. Lancaster, PA:
DEStech Publications, Inc.

REPORT DOCUMENTATION PAGE				Form Approved OMB No. 0704-0188	
<p>Public reporting burden for this collection of information is estimated to average 1 hour per response, including the time for reviewing instructions, searching existing data sources, gathering and maintaining the data needed, and completing and reviewing the collection information. Send comments regarding this burden estimate or any other aspect of this collection of information, including suggestions for reducing the burden, to Department of Defense, Washington Headquarters Services, Directorate for Information Operations and Reports (0704-0188), 1215 Jefferson Davis Highway, Suite 1204, Arlington, VA 22202-4302. Respondents should be aware that notwithstanding any other provision of law, no person shall be subject to any penalty for failing to comply with a collection of information if it does not display a currently valid OMB control number.</p> <p>PLEASE DO NOT RETURN YOUR FORM TO THE ABOVE ADDRESS.</p>					
1. REPORT DATE (DD-MM-YYYY) May 2012		2. REPORT TYPE Reprint		3. DATES COVERED (From - To)	
4. TITLE AND SUBTITLE Results and Analysis from Mine Impulse Experiments Using Stereo-Digital Image Correlation				5a. CONTRACT NUMBER	
				5b. GRANT NUMBER	
				5c. PROGRAM ELEMENT NUMBER	
6. AUTHOR(S) Craig Barker, Douglas Howle, Terry Holdren, Jeffrey Koch, and Raquel Ciappi				5d. PROJECT NUMBER	
				5e. TASK NUMBER	
				5f. WORK UNIT NUMBER	
7. PERFORMING ORGANIZATION NAME(S) AND ADDRESS(ES) U.S. Army Research Laboratory ATTN: RDRL-SLB-E Aberdeen Proving Ground, MD 21005				8. PERFORMING ORGANIZATION REPORT NUMBER ARL-RP-0370	
9. SPONSORING/MONITORING AGENCY NAME(S) AND ADDRESS(ES)				10. SPONSOR/MONITOR'S ACRONYM(S)	
				11. SPONSOR/MONITOR'S REPORT NUMBER(S)	
12. DISTRIBUTION/AVAILABILITY STATEMENT Approved for public release; distribution unlimited.					
13. SUPPLEMENTARY NOTES This article appeared in its original form in 26th International Ballistics Symposium, 2011. Lancaster, PA: DEStech Publications, Inc.					
14. ABSTRACT This paper focuses on the development and analysis of experimental mine impulse data for simple v-shaped structures constructed with a top floor plate. The impulse data were collected at a small-scale test facility designed and operated by the U.S. Army Research Laboratory (ARL) Weapons and Materials Research Directorate (WMRD). The facility uses stereo-digital image correlation to track the motion of a speckled pattern painted on the top floor plate of the target. This capability allows for the measurement of the vibration motion of the top floor plate from which the global motion of the target can also be derived. Experiments were performed using three v-shaped targets with angles of 10, 20 and 30 degrees. Centerline shots were performed on each structure using two cylindrical C-4 charge sizes, 600g and 800g, each with a 1:3 height-to-diameter ratio. Off-center shots were performed for the 20 degree target with C-4 charge sizes of 800g and 1000g. Finite element modeling and statistical analysis of the experimental data was performed by the Survivability Lethality Analysis Directorate (SLAD) of ARL.					
15. SUBJECT TERMS Mine, impulse, digital image correlation					
16. SECURITY CLASSIFICATION OF:			17. LIMITATION OF ABSTRACT UU	18. NUMBER OF PAGES 18	19a. NAME OF RESPONSIBLE PERSON Craig Barker
a. REPORT Unclassified	b. ABSTRACT Unclassified	c. THIS PAGE Unclassified			19b. TELEPHONE NUMBER (Include area code) (410) 278-0214

Results and Analysis from Mine Impulse Experiments
Using Stereo-Digital Image Correlation

Craig Barker¹
Douglas Howle¹
Terry Holdren¹
Jeffrey Koch²
Raquel Ciappi³

This paper focuses on the development and analysis of experimental mine impulse data for simple v-shaped structures constructed with a top floor plate. The impulse data were collected at a small-scale test facility designed and operated by the U.S. Army Research Laboratory (ARL) Weapons and Materials Research Directorate (WMRD). The facility uses stereo-digital image correlation to track the motion of a speckled pattern painted on the top floor plate of the target. This capability allows for the measurement of the vibration motion of the top floor plate from which the global motion of the target can also be derived. Experiments were performed using three v-shaped targets with angles of 10, 20 and 30 degrees. Centerline shots were performed on each structure using two cylindrical C-4 charge sizes, 600g and 800g, each with a 1:3 height-to-diameter ratio. Off-center shots were performed for the 20 degree target with C-4 charge sizes of 800g and 1000g. Finite element modeling and statistical analysis of the experimental data was performed by the Survivability Lethality Analysis Directorate (SLAD) of ARL.

BACKGROUND

Improvised explosive devices and other traditional under-body blast weapons are a significant threat to military ground vehicle systems. Engineers and scientists attempting to analyze the effects of under-body blast events have an array of commercial and internally-developed tools at their disposal, each with its own set of limitations. Finite element (FE) models offer the capability to evaluate the entire event sequence from the detonation of the buried explosive to the response of the occupant. However, FE models for full system-level mine events require significant time for input preparation, debugging and computation. Current experience for modeling system-level events using LS-DYNA® [1] indicates computation times can exceed 100 hours using high performance computing assets. These run times include a detailed vehicle model, multiple anthropomorphic test devices and use of the Arbitrary Lagrangian-Eulerian (ALE) fluid-structure interaction (FSI) [2,3] capability within LS-DYNA to model the soil, air and explosive.

¹ Director, U.S. Army Research Laboratory, (RDRL-SLB-E), APG, MD, 21005, U.S.A.

² Director, U.S. Army Research Laboratory, (RDRL-WMP-G), APG, MD, 21005, U.S.A.

³ SURVICE Engineering Company, 4695 Millennium Dr., Belcamp, MD, 21017, U.S.A.

Computational times can be significantly reduced if simplified air-blast loading approaches are used to estimate the mine blast load. Current approaches may improve efficiency, but require significant engineering judgment for proper application. Regardless of the selected loading approach, LS-DYNA has not undergone a formal verification, validation, and accreditation (VV&A) process for application to under-body blast events. In fact, no end-to-end under-body blast model or methodology currently exists that has been subjected to the rigorous VV&A process required for use in U.S. Army evaluations. The U.S. Army Research Laboratory therefore initiated a multi-agency effort to develop an under-body blast methodology (UBM) primarily to support the test and evaluation (T&E) process for Army ground vehicle systems. The general goal of the UBM project is to develop a robust modeling capability that is accurate, efficient and flexible enough to support an array of under-body engagement conditions. Secondly, the methodology may be used to support Army force-level modeling, general analyses of alternatives, and vehicle design studies.

Various models, tools, techniques and methodologies exist to evaluate different technical aspects of an under-body blast event. The primary technical areas for an under-body blast event are depicted in Figure 1. The UBM effort is evaluating existing models, or developing new methods, to address each of the technical elements. The effort includes evaluation of both high-resolution (HR) physics models and reduced-order (RO) engineering models. The UBM development process leverages existing organizational competencies to follow a parallel development process for both HR and RO capabilities. The ultimate vision is one model or methodology that can support a variety of applications.

One key aspect of the UBM project is the assessment and validation of models used to predict the loading from a mine blast event. Controlled experimental data is therefore required not only for validation of models, but also to establish the inherent variability of impulse. This paper focuses on analysis and preliminary modeling of data generated from sub-scale impulse experiments for simple v-angle structures constructed with a top floor plate.

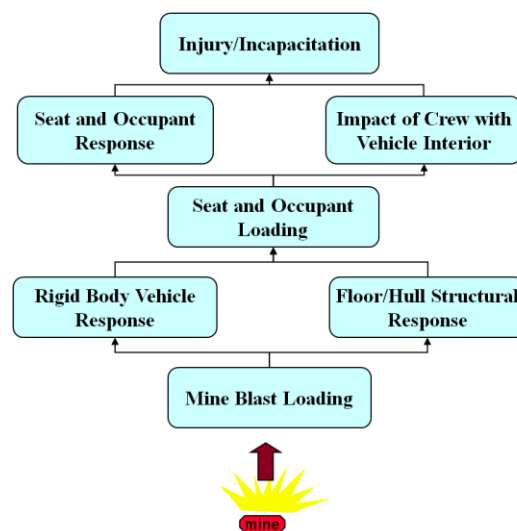


Figure 1. UBM project technical elements.

EXPERIMENTAL SETUP

The experiments were conducted at a WMRD facility used for sub-scale mine impulse testing. The facility uses a buried steel-walled box that is 6 ft x 6 ft with a depth of 4.5 ft, referred to as the “Sandbox”. The Sandbox has a 1 kg explosive capacity and can be filled with any desired soil type. Targets are placed on angle iron rails resting on supports at both ends of the box. The supports are adjusted to achieve the desired standoff from the top surface of the soil. Figure 2 illustrates the general experimental setup. A high-speed camera located at ground level is used to observe the trajectory of a target. The motion of points on the top plate is acquired using two stereo high-speed cameras situated atop a nearby tower.

Target Geometries

The experiment compared different target geometries subjected to a buried charge. The basic target design was a V-shape, composed of A-36 Mild Steel. The majority of the target was a hollow box with a height $H=50.8$ mm, and length $L=700$ mm, and a width $W=700$ mm. The bottom side protruded out in a “V” shape with an angle Θ . The three variations of the target geometry are values for the angle Θ of 10 deg, 20 deg, and 30 deg. Once placed on the steel rails, each target had a standoff of 248.92 mm, measured from the spine of the “V” to the surface of the soil.

Soil Bed

The soil used was a sand-clay mixture. For each shot the Sandbox was filled and lightly tamped. Before detonation, a densitometer was used to determine the dry density, wet density, and moisture of the soil. Readings were taken at three locations, the center of the box and two locations 304.8 mm away in opposite directions from the center. After all measurements were taken, the charge was put into place.

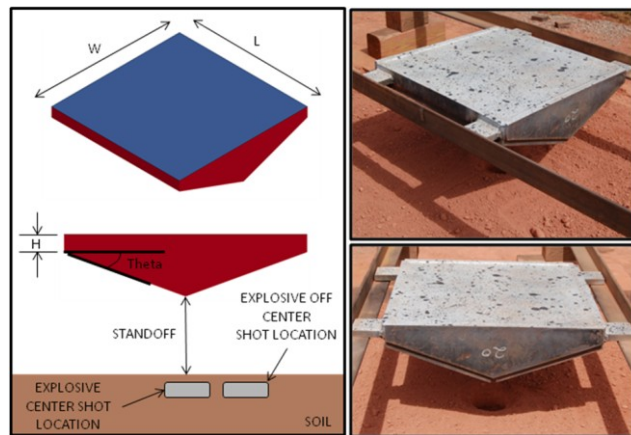


Figure 2. General experimental setup.

High Explosive Charge

The charge used for all experiments was buried C4. The explosives were hand-shaped into cylinders with a 1:3 height to diameter ratio. Centerline shots were conducted with charge sizes of 600g and 800g. Off-center shots conducted at 600g, 800g, and 1000g and these charges were located midway between the spine of the “V” and the outermost edge of the target. Overburden, measured from the top of the C4 to the surface of the soil, was held constant for each shot. Each charge was bottom-detonated with an RP-83 detonator.

Experimental Data Acquisition

Target motion data was acquired using two high-speed cameras and was processed with stereo-digital imaging correlation software. The cameras were synchronized so that they recorded the event identically from two different positions. A speckled pattern on the surface of the target provided the software with a way to track its motion as the speckle marks shifted pixels. The software used the pixel tracking to determine the rigid motion of the target and produce a strain field of the target’s top surface. This information was used to determine the impulse imparted on the target and the oscillatory motion of the target’s top surface.

In order to determine the global motion of the target, the equation of a plane (Equation 1) was used.

$$a(x_2 - x_1, y_2 - y_1, z_2 - z_1) + b(x_3 - x_1, y_3 - y_1, z_3 - z_1) = (x_{cp} - x_1, y_{cp} - y_1, z_{cp} - z_1) \quad (1)$$

The first step was to solve for variables a and b in the equation for a plane using known points in a static situation to determine the relationship between rigid edge points and some center point, CP. Figure 3 illustrates the top plane of the target at two different time steps. CP represents a rigid center location free of oscillation. As the edge points moved, the solved equation for a plane was used to determine the new location of the rigid center point, CP. The cameras also tracked the location of this point, CP, however, its time history captured the oscillations of the surface at this location. One method of estimating the impulse delivered to the target is to assume a truly impulsive load delivery and then solve the kinematic equations of motion.

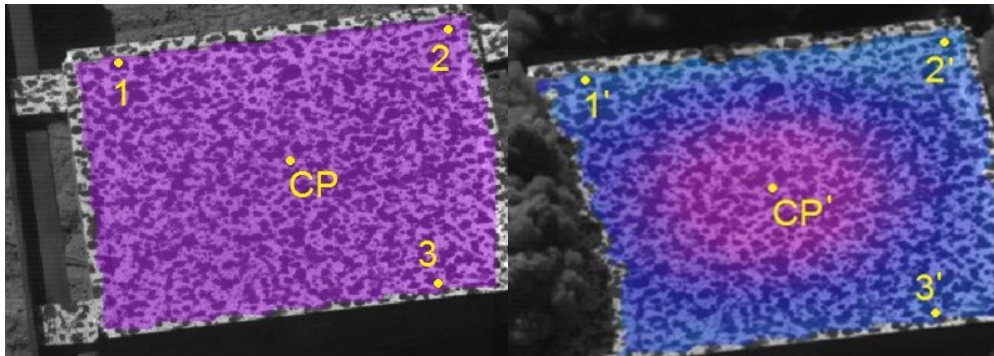


Figure 3. Top view of target plate.

The velocity of the plate center point for each time step can be estimated by recasting the equations of motion in the form of Equation 2.

$$v_n = \frac{(Z_{CP,n} - Z_{CP,i}) + 0.5g(t_n - t_i)^2}{(t_n - t_i)} \quad (2)$$

where,

Z_{CP} = Z coordinate of CP

v = velocity

t_i = initial time

t = time

n = frame number

g = gravitational acceleration

The initial velocity, v_i , of the target can be determined by using Equation 3 at each successive time step. The impulsive velocity will be the steady-state value to which $v_{i,n}$ will converge.

$$v_{i,n} = \sqrt{v_n^2 - 2gZ_{CP,n}} \quad (3)$$

Impulse is a measurement of the change in momentum, and therefore the vertical impulse, I_n , can be found by multiplying the mass of the target by its initial vertical velocity (Equation 4).

$$I_n = m_{target} \times v_i \quad (4)$$

It should be noted that the forces take time to be fully applied to the target. Assuming that some acceleration was observed, the values of v_i , calculated from Equation 3, change from frame to frame. As stated, the values show steady results when the forces were fully applied and at sufficient times, t_n , when the impulsive assumption becomes more valid. Due to obscuration of the target with dirt particles and computational limitations of this technique, subjective engineering judgment must be applied in the estimation of the final total impulse. As an alternative calculation of total impulse, the rigid-body displacement of CP was plotted as a function of time and the derivative of a linear trend at the initial time was taken as an estimate of v_i . Equation 4 was then applied to estimate the total impulse. This method was considered less subjective for estimating total impulse than choosing the maximum value from the computation of impulse for each time step. All data presented in the results and analysis section are based on this approach, however, both approaches yielded comparable results.

The oscillatory motion of the top surface of the target was determined using a combination of output from the software and the already determined rigid motion of the target. The motion of the surface was oscillating while the target was moving upward. Therefore, the data for the rigid motion of the target were subtracted from the data for the motion of the center of the surface, which provided the purely oscillatory portion of the motion.

EXPERIMENTAL RESULTS AND ANALYSIS

The experimental data for the centerline and off-center shots are presented in Table I and Table II, respectively. Data for shots 3, 7, and 20 were not captured resulting in a total of 21 available data points for analysis. The normalized impulse is plotted in Figure 4 for the centerline shots. As anticipated, the data exhibit a decreasing trend with increasing target angle due to the effects of the geometry. The data exhibit a reasonable variability based on subjective judgment of the magnitude of the standard errors presented in Table I. The standard error is defined as the sample standard deviation divided by the square root of the sample size. However, it should be noted that the sample size is very small and may underestimate the population standard error.

TABLE I. IMPULSE DATA FOR CENTERLINE SHOTS.

Shot #	Target Angle (deg)	Charge Size (g)	Normalized Impulse	Mean	Standard Error
1	20	600	0.795	0.780	0.028
2	20	600	0.864		
4	20	600	0.841		
5	20	800	0.683		
6	20	800	0.777		
8	20	800	0.720		
9	10	600	1.000	0.952	0.025
10	10	600	0.963		
11	10	600	0.883		
12	10	600	0.961		
13	30	600	0.679	0.598	0.024
14	30	600	0.577		
15	30	600	0.596		
16	30	600	0.579		

TABLE II. IMPULSE DATA FOR OFF-CENTER SHOTS.

Shot #	Target Angle (deg)	Charge Size (g)	Normalized Impulse	Mean	Standard Error
17	20	800	0.765	0.754	0.048
18	20	800	0.735		
19	20	800	1.003		
21	20	600	0.778		
22	20	1000	0.647		
23	20	1000	0.740		
24	20	1000	0.612		

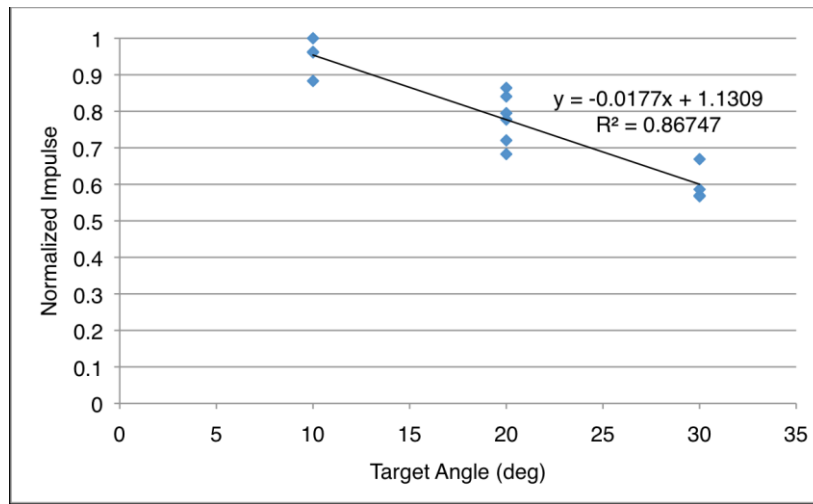


Figure 4. Normalized impulse vs. target angle.

Statistical Analysis

It was desired to perform a formal statistical analysis of the entire data set without the potential bias of engineering expectations. The dependent variable was the observed impulse. The independent variables chosen for analysis were target angle, target mass, charge mass, soil moisture, and charge offset. Table III displays the correlation matrix for the variables including observed impulse. This value can range from -1 to 1 with a value of 1 representing a strong positive linear relationship and -1 representing a strong inverse (negative) linear relationship. A positive linear relationship indicates that as one variable increase the other tends to increase. Conversely, a negative linear relationship indicates that as one variable increases the other tends to decrease. Note that this matrix is symmetric, and only the bottom diagonal values are shown. Target mass is highly correlated with target angle (0.99) because the mass of the structure increased as the target angle increased. The target angle, rather than target mass, was chosen for the development of the statistical model.

Observing only the correlation coefficient between charge offset and impulse (0.52), one might conclude that as charge offset increases, observed impulse increases. However, charge offset is highly correlated with charge mass (0.69). This is because the offset shots were conducted with 800 g and 1000 g charges in

TABLE III. CORRELATION MATRIX.

	Impulse	Charge mass	Target mass	Target angle	Charge offset	Soil moisture
Impulse	1.00					
Charge mass	0.69	1.00				
Target mass	-0.58	-0.07	1.00			
Target angle	-0.52	0.00	0.99	1.00		
Charge offset	0.52	0.69	-0.06	0.00	1.00	
Soil Moisture	0.19	-0.09	-0.13	-0.15	-0.28	1.00

all but one event, which was a 600 g charge. Eleven of the centerline shots were conducted with 600 g charges and 3 were 800 g charges. Any increase in the overall average impulse for the offset shots is more likely the cause of the larger charge masses. To test this hypothesis, a two sample t-test was conducted on the mean observed impulse for the 20° target and 0.8 kg charge shots for both the centerline and offset configurations. Using $\alpha = 0.05$ significance level, the mean observed impulse for the centerline and offset shots were not found to be significantly different (p-value = 0.62, this value would need to be less than 0.05 to be statistically significant). A p-value is the probability that a result obtained in a statistical test is due to chance. A small p-value indicates that it is very unlikely that the results were due to chance. In this test, the data collected is insufficient to show that offset shots result in statistically different observed impulse values than the centerline shots. It is not the intention to rule out offset as a significant contributor to impulse. However, with the data collected a difference in impulse for offset shots cannot be shown. With additional data this difference may become apparent. In particular, data from offset shots with 10° and 30° degree angles and centerline data with 1.0 kg charge masses would be useful.

Multiple regression was used to determine if the observed impulse could be adequately predicted using the variables of charge mass, target angle, soil moisture, and offset. After initial evaluation it appeared that one of the events had an unusually large observed impulse when compared to a similar event. Any attempt at finding a well-fitting multiple regression model was greatly hindered when including this data point. Because it was a highly influential point, it was left out of the regression model. Surprisingly, charge offset was not found to be a significant variable ($\alpha = 0.05$, p-value = 0.71) and was removed from the main effects model. Once removed the p-value for soil moisture was 0.06. Although this value is not less than the $\alpha = 0.05$ significance level set prior to the test, it is borderline significant and the decision was made to leave soil moisture in the model. Charge mass and $\cos(\text{target angle})$ are highly significant with p-values less than 0.0000. These results are shown in TABLE IV. The resulting model can be seen in Figure 5 and was found to provide the best fit (adjusted R-squared = 0.88 – a very good fit). A common interpretation of an R-squared value would be that this model explains 88% of the expected variation in the observed impulse. The cosine of the target angle was used in the model. Using this transformation provided a slightly better fit (0.88 vs. 0.85). The events where the charge was offset are circled on the plot.

TABLE IV. STATISTICAL PARAMETERS FOR IMPULSE MODEL.

	t-value	p-value
Intercept	-6.8877	0.0000
Charge mass	8.2572	0.0000
Cos(target angle)	7.2310	0.0000
Soil moisture	2.0132	0.0612

Predicted Impulse

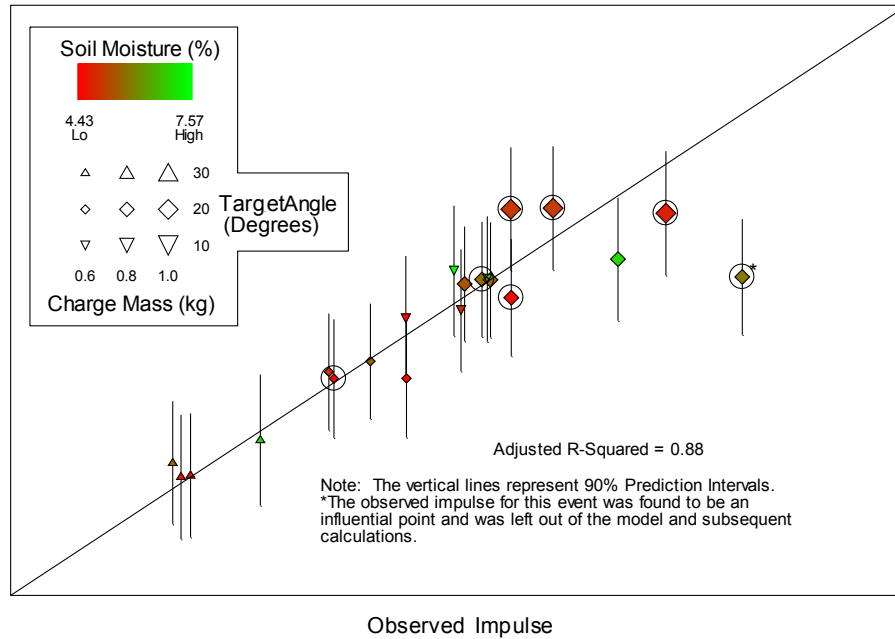


Figure 5. Main effects impulse model.

PRELIMINARY FINITE ELEMENT MODELING

The LS-DYNA finite element code was used to simulate the mine blast loading and structural response for the various target geometries. Historically, mine blast loads have been simulated in LS-DYNA using the ALE method or the ConWep [4,5] air-blast loading model implemented by Randers-Pehrson & Bannister [6]. Since ConWep is an air-blast loading model, the pressure loading time history, or charge mass, must be scaled by a factor in order to simulate the additional impulse on the structure caused by the interaction of the soil and structure.

There are advantages to using the air-blast loading model because it's easy to use and quick running. However, the factors which must be used to scale the peak pressure or charge mass are not easily predicted. In order to find factors to match total impulse for each shot number, a baseline LS-DYNA model was run using the test charge mass and a unit scale factor applied to the peak pressure time history load curve. The total impulse from the baseline run was used to guide systematic model runs aimed at simply matching the estimated test impulse by adjusting the user-defined scale factor.

For dynamic response of the top plate, the target meshes, composed of fully integrated shell elements, were refined until convergence of the structural displacements and velocities was achieved. A simplified version of the Johnson Cook material model was used since the targets were subjected to high strain rates. The simplified Johnson Cook material model implemented in LS-DYNA does not account for the effect of temperature changes on the material. Since the default number of shell element integration points was used, a resultant plasticity formulation was activated in the simplified Johnson Cook model [3].

The normalized ConWep scale factors required to reasonably match the experimental impulse for seven shots are presented in TABLE V. Modeling of the remaining shots will be completed in the future. Additional model runs could be made to obtain a closer match between the experimental and impulses, but this was not considered necessary at this time. After finding air-blast pressure scaling factors to match total impulse on the structures, attention was turned toward comparing the measured and modeled target structural responses. Comparing the rigid body motion measured during the test and that predicted by the model was a trivial task since the total structural impulse and mass matched between the model and test. The deflection of the center of the plate was of more interest than the rigid-body motion, and was compared between the models and tests. Figure 6 displays an example of the difference between the model and test center plate displacements for shot number 1. In addition to the center plate displacements, the center plate velocities are of interest in this investigation. Figure 7 illustrates the model and test center plate velocities for shot number 1.

TABLE V. CONWEP SCALE FACTORS.

Shot #	Charge Size (g)	Target Angle (deg)	Normalized Test Impulse	Normalized Model Impulse	Normalized Scale Factor
1	600	20	0.795	0.796	0.920
2	600	20	0.864	0.864	1.000
4	600	20	0.841	0.835	0.967
6	800	20	0.777	0.777	0.965
13	600	30	0.679	0.675	0.995
15	600	30	0.596	0.585	0.920
16	600	30	0.579	0.569	0.920

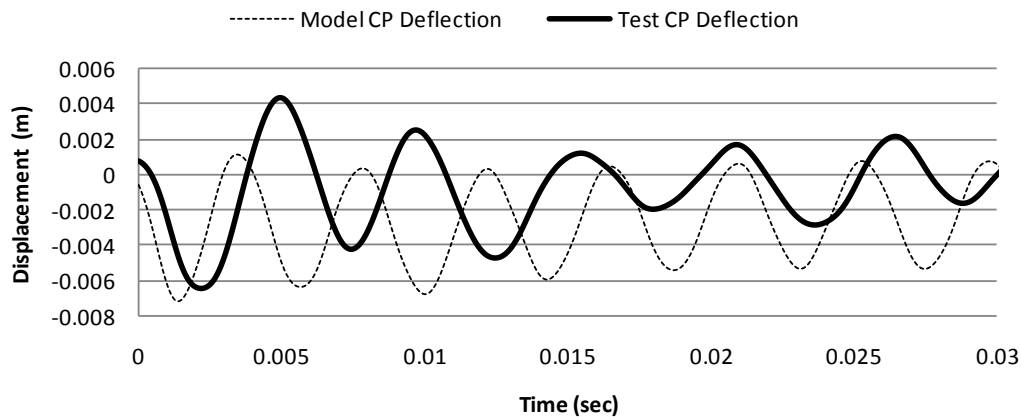


Figure 6. Comparison of center point displacements for shot 1.

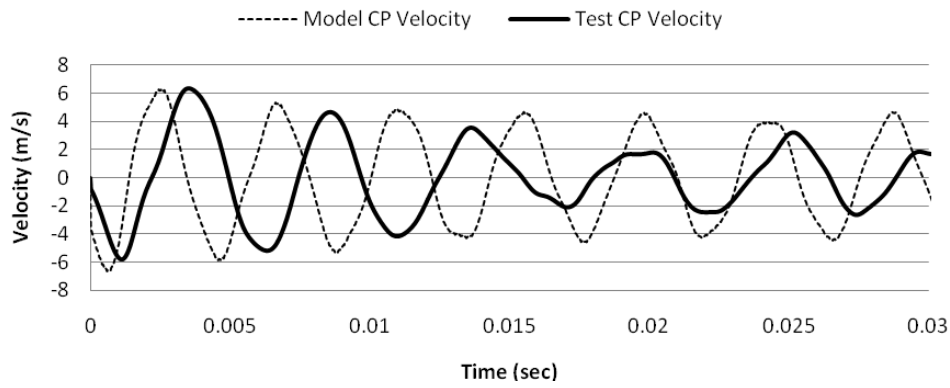


Figure 7. Comparison of center point velocities for shot 1.

To ensure the model and test data was compared properly, the same process was used to analyze the test and model data. Both the experimental time history traces and the model time history traces were filtered with an SAE 180 Hz filter. The filter selection was based on the fact that it provided clean results that did not appear to affect the fundamental vibration mode of the target center point. The only concern with filtering the test and model data is the apparent shift from zero that it caused in the center plate position time histories for the model and test results. Assuming this error or offset is constant throughout the time history, it is expected to be removed when taking the derivative of the test and model position time histories.

The peak value of the center plate oscillatory velocity is of primary concern to the authors. The experimental error between the test and model predicted velocity is 0.75% for shot number 1.

SUMMARY

Vibratory plate motion was recorded using stereo-digital image correlation and impulse loads were estimated from those measurements. This technique was relatively new in its development for this purpose at ARL/WMRD's sub-scale impulse facility. Since this was the only measurement technique used for the experiments, there was no opportunity for alternative measurement comparisons. However, the impulse trends were generally consistent with engineering expectations and knowledge of historical impulse tests conducted at ARL/WMRD and other facilities. Variability of the impulse for repeat experiments was considered reasonable based on knowledge of similar test events, but sample sizes were relatively small. Independent statistical analysis of the data yielded a main effects model with an adjusted R-squared value of 0.88. In other words, 88% of the variability in observed impulse can be explained by the model and controlled with adequate test procedures. The main effects model did indicate that the off-center charge location was not significant which is counter-intuitive for v-shaped targets. It should be noted that the off-center shot locations resulted in increased obscuration of the target by the soil particles. This limited the points on the top plate available for tracking by the high-speed cameras and could increase the uncertainty in the computed impulse estimates for the off-center shots. However,

errors associated with the measurement technique have not yet been quantified. Finally, preliminary finite element modeling results were presented. Conclusions related to model results will follow upon future completion of the effort.

RECOMMENDATIONS

The data set presented here, established for a relatively simplified target design, support a building block approach for model validation that will ultimately extend to a full system-level VV&A for ground vehicle systems. Future experimental programs should leverage the knowledge gained here to better establish a more robust experimental design. The finite element modeling analysis should be completed with both the simplified ConWep air-blast loading approach as well as the more complex ALE approach. Consideration should be given to adding additional measurement techniques to supplement the stereo-digital image correlation. This would add further confidence to the technique. Full-scale tests should be performed on similar geometries to address the issue of scalability. Finally, additional experimentation must be conducted with varying soil types, soil moisture levels, explosive types, charge burial depths, and more complex geometries to establish a robust data set.

REFERENCES

1. LS-DYNA version 971, Livermore Software Technology Corporation, Livermore, CA. (LS-DYNA is a registered trademark of Livermore Software Technology Corporation)
2. Hallquist, John O., LS-DYNA Theoretical Manual, Livermore Software Technology Corporation, Livermore, CA, March 2006.
3. LS-DYNA Keyword User's Manual (Version 971), Livermore Software Technology Corporation, Livermore, CA, May 2007.
4. Department of the Army. "Fundamentals of Protective Design for Conventional Weapons." TM 5-855-1, Washington, D.C., November 1986.
5. Kingery, C.N. and G. Bulmash. "Air-Blast Parameters from TNT Spherical Air Burst and Hemispherical Surface Burst." ARBRL-TR-02555, U.S. Army Ballistic Research Laboratory, Aberdeen Proving Ground, MD, April 1984.
6. Randers-Pehrson, G. and K. Bannister. "Airblast Loading Model for DYNA2D and DYNA3D." ARL-TR-1310, U.S. Army Research Laboratory, Aberdeen Proving Ground, MD, March 1997.

NO. OF COPIES	ORGANIZATINO	NO. OF COPIES	ORGANIZATINO
1 ELEC	ADMNSTR DEFNS TECHL INFO CTR ATTN DTIC OCP 8725 JOHN J KINGMAN RD STE 0944 FT BELVOIR VA 22060-6218	3	US ARMY RSRCH LAB ATTN RDRL WMP G S KUKUCK ATTN RDRL WMP F E FIORAVANTE ATTN RDRL WMP G N ELDREDGE BLDG 309 ABERDEEN PROVING GROUND MD 21005-5066
1	U.S. ARMY RSRCH LAB ATTN RDRL SLB S S SNEAD BLDG 247 ABERDEEN PROVING GROUND MD 21005-5068	2	US ARMY RSRCH LAB ATTN RDRL SLB D L MOSS ATTN RDRL SLB D R GROTE BLDG 1068 ABERDEEN PROVING GROUND MD 21005-5068
1	US ARMY MATERIEL SYS ANALYSIS ACTIVITY MINE & IED ANALYSIS TEAM ATTN RDECOM AMSAA M SCHUMACHER ABERDEEN PROVING GROUND MD 21005	4	US ARMY RSRCH LAB ATTN RDRL SLB E M MAHAFFEY ATTN RDRL SLB E D HOWLE ATTN RDRL SLB E D LYNCH ATTN RDRL SLB A M PERRY BLDG 328 ABERDEEN PROVING GROUND MD 21005-5068
3	US ARMY RDECOM-TARDEC ATTN RDTA RS J SHENG ATTN RDTA RS M VUNNAM ATTN RDTA RS MS 157 R THYAGARAJAN 6501 E ELEVEN MILE RD WARREN MI 48397-5000	1	US ARMY RSRCH LAB ATTN RDRL SLB W L ROACH BLDG 390A ABERDEEN PROVING GROUND MD 21005-5068
1	SURVICE ENGRG ATTN D VAN DUSEN 4695 MILLENIUM DR BELCAMP MD 21017-1505	1	US ARMY RSRCH LABORATORY ATTN RDRL SLB G P MERGLER BLDG 247 ABERDEEN PROVING GROUND MD 21005
5	US ARMY RSRCH LAB ATTN RDRL SLB D J GURGANUS ATTN RDRL SLB D T HOLDREN ATTN RDRL SLB E C BARKER ATTN RDRL SLB E P HORTON ATTN RDRL SLB E R CIAPPI ABERDEEN PROVING GROUND MD 21005	3	US ARMY RSRCH LAB ATTN IMNE ALC HRR MAIL & RECORDS MGMT ATTN RDRL CIO LL TECHL LIB ATTN RDRL CIO LT TECHL PUB ADELPHI MD 20783-1197
2	US ARMY RSRCH LAB ATTN RDRL WMP F S TROMBETTA ATTN RDRL WMP G J KOCH ABERDEEN PROVING GROUND MD 21005		